2016

Heat Transfer and Visualization in Large Flattened-Tube Condensers with Variable Inclination

William A. Davies
ACRC, University of Illinois, United States of America, daviesi2@illinois.edu

Yu Kang
ACRC, University of Illinois, United States of America, yukang2@illinois.edu

Pega Hrnjak
pega@illinois.edu

Anthony M. Jacobi
ACRC, University of Illinois, United States of America, a-jacobi@illinois.edu

Heat Transfer and Visualization in Large Flattened-Tube Condensers with Variable Inclination

William A. DAVIES[1], Yu KANG[1], Pega HRNJAK[1,2]*, Anthony M. JACOBI[1]

[1]University of Illinois at Urbana-Champaign,
Department of Science and Engineering,
Urbana, IL, USA
daviesi2@illinois.edu, yukang2@illinois.edu, pega@illinois.edu, a-jacobi@illinois.edu

[2]Creative Thermal Solutions,
Urbana, IL, USA

* Corresponding Author

ABSTRACT

An experimental study of convective condensation of steam in a large, inclined, finned tube is presented. This study extends previous work in the field on inclined, convective condensation in small, round tubes to large, non-circular tubes with low inlet mass flux of vapor. The steel condenser tube in this study was designed for use in a power-plant air-cooled-condenser array with forced convection of air. The tube was cut in half lengthwise and covered with a polycarbonate viewing window to allow simultaneous visualization and heat transfer measurements. The half tube test section had inner dimensions of 214 mm x 6.3 mm and a length of 10.72 m. This study investigated heat transfer results for a mass flux of steam of 6.8 kg/m^2-s over a range of inclination angles. The angle of inclination of the condenser tube was varied from 0.3^o (horizontal) to 13.2^o downward flow. The experiments were performed with uniform crossflowing air with velocity of 2.0 m/s. Both dropwise and filmwise condensation were observed on the tube wall, and depth of the condensate river at tube bottom was seen to decrease with an increase in inclination angle. Average steam-side heat transfer coefficient was shown to increase with an increase in inclination angle. However, average steam-side heat transfer coefficient was much lower than the predictions of both vertical flat-plate Nusselt condensation, as well as Kroger's correlation for condensation in air-cooled condensers. Overall, the results suggest that an improvement in steam-side heat transfer performance can be achieved by varying the tube inclination angle. Pressure drop results are presented in a companion paper.

1. INTRODUCTION

This study investigates an inclined, flattened tube with internal convective condensation in both dropwise and filmwise modes, with a focus on air-cooled condenser (ACC) applications for power plants. Each of these physical aspects and phenomena have been studied individually, but never in this combination. Due to the large, flat surface area of the condenser and the low vapor velocity of the steam, the classical film condensation model presented by Nusselt (1916) serves as a lower bound for heat transfer. Nusselt's model assumes laminar film condensation and gravity-driven flow, and yields a mean heat transfer coefficient (HTC) over a flat plate of:

$$\bar{h} = 0.943 \left[\frac{i_{fg} \rho_f (\rho_f - \rho_g) g k_f^{\,3}}{W \mu_f (T_{sat} - T_w)} \right] \quad (1)$$

For flow through ducts, heat-transfer correlations are more commonly used, however. The correlations by Shah (1979), Soliman et al (1968), Traviss et al (1972) and Chato (1960) are among the most-commonly used of these. However, all of these are for round tubes. The correlation of Chato is most applicable to this investigation, because it models separated flow at low mass fluxes. Chato predicted that heat transfer through the laminar condensate layer would be negligible compared to that along the condenser wall. Therefore, heat transfer will decrease as the thickness of this

layer increases. Chato also applied his model to an inclined tube, where it showed an increase in HTC as the tube was inclined downward from the horizontal, but a decrease in HTC upon reaching a critical inclination angle.

Several more-recent studies have investigated downwardly-inclined condensation in short, cylindrical tubes. Lips and Meyer (2012), Noie et al., (2007), and Lyulin et al. (2011) have shown that HTC at first increases for an increasing inclination angle in downward flow. After reaching a critical angle, HTC then decreases steadily until vertical downward flow is reached. In their study with R134a in an 8.38mm diameter tube, Lips and Meyer showed that the optimum inclination angle for HTC occurred between 15° and 30°. Noie et al. studied an inclined thermosiphon with a diameter of 14.5mm and water as the working fluid. They found a similar result with 15-60° as the optimum angle. Lyulin et al. studied low mass flux of condensing ethanol in a 4.8mm tube, and found a maximum HTC between 15 and 35° inclination. In a more recent study, Olivier et al. (2015) expanded on the study of Lips and Meyer (2012) to conclude that for low mass flux and quality, HTC and void fraction reach a maximum at 10-30° inclination in downward condensing flow.

In a slight departure from the above studies, Wurfel et al., (2003) used a larger, 2cm tube with n-heptane in shear-dominated flows, and found that HTC increased with increasing inclination angle, reaching a maximum at vertical downward flow. In a complete departure, Akhavan –Behabadi et al., (2007) found that HTC decreased for all downward inclination angles. They used R134a with high mass fluxes, but in a microfin tube.

In an analytical analysis, Kröger (2004) developed a correlation specifically for inclined ACC condensers:

$$Nu_c = 1.197(sin\varphi)^{0.1755}\left(\frac{\rho_c}{\mu_c}\right)^{0.5}\left(\frac{\mu_g}{\rho_g}\right)^{0.5} Re_{gi}^{0.325} \quad (2)$$

The previous work by Wang and Du (2000) clarifies these mixed results by presenting experimental results for a range of small-diameter tubes at a range of mass fluxes and qualities. Their results showed an increase in HTC for increasing inclination in smaller tubes. For larger tubes, HTC only increased at low qualities, and HTC averaged across all qualities decreased. Overall, the experimental investigations have produced mixed results, showing that the effect of inclination is moderated by other variables, most notably tube diameter, vapor quality and mass flux. In general, for large tubes, and low quality and mass flux, condensation heat transfer coefficient has been shown to at first increase with increasing inclination angle, then decrease after reaching a critical angle.

Other authors have provided further insight by measuring related parameters in inclined tubes. Cheng et al. (2015) used a numerical model to predict film condensation in a flattened ACC tube for tube inclination angles varying from 5 to 85°. They predicted that the maximum depth of the condensate river at the tube bottom would vary from 2.1 to 0.8 mm, corresponding to an increase in the tube inclination angle.

In order to clarify these mixed results for the specific application of large, flattened-tube air-cooled condensers, this study aimed to measure steam-side heat transfer coefficient at multiple downward inclination angles and explain those results with the aid of visualization.

2. EXPERIMENT DESCRIPTION

2.1 Facility

The concept of the investigation was to measure the internal, convective, condensation heat transfer on the surface of one of the tubes from an ACC array. The tube was cut in half lengthwise to allow visualization of the flow pattern through a transparent wall while simultaneously measuring heat transfer and pressure drop. The tube was placed in a structure that could rotate from the horizontal position (0° inclination) to vertical (90° inclination) to experimentally determine the effect of inclination on heat transfer, pressure drop and flow regime. Air flow was provided by 134 small axial fans that allowed variation of the velocity of air and measurement of its effect.

This complex approach came with certain compromises. The most obvious was the addition of the transparent wall for visualization. It reduced by half the flow area for vapor and condensate. However, the quantity of vapor and condensate were also reduced compared to a full tube, so the mass flux and flow regimes remained unchanged. Another compromise was the accuracy of determining the local heat transfer coefficient on the steam side. The local

HTC was based on wall temperature measurements. The T-type (CuCo) thermocouple probes used have limited accuracy and the measurement was complicated by the difficulty in reading actual wall temperature. The secondary determination approach was also problematic in that it was based on the assumption that the air side was well known.

The experimental facility is presented in Figure 1 schematically and with accompanying photograph.

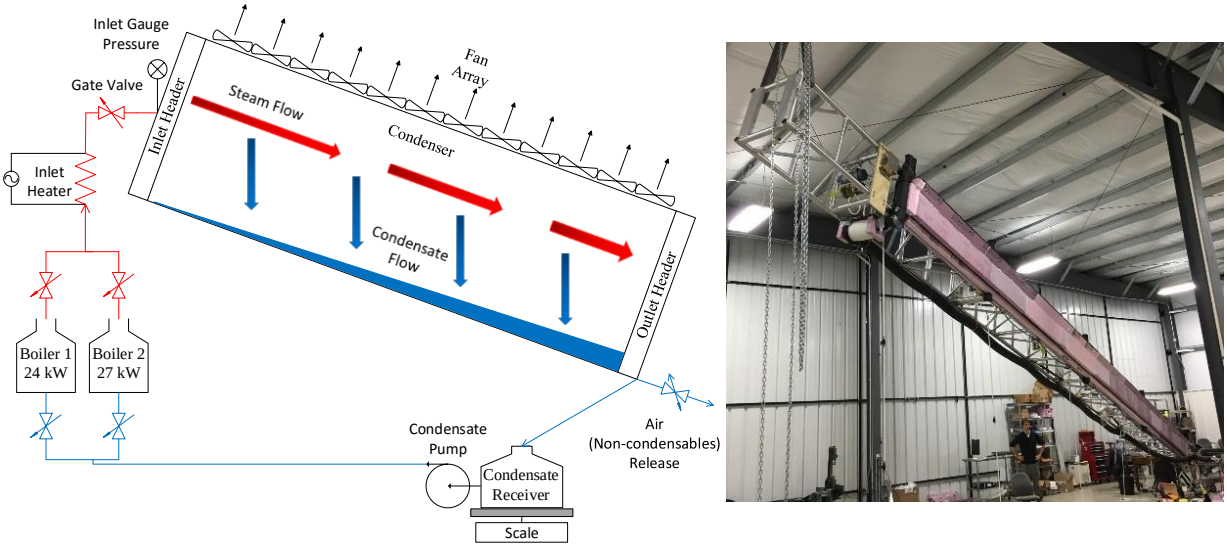

Figure 1: Schematic drawing and photograph of the experimental facility

Steam was provided to the condenser by two boilers controlled by solid-state controllers, with a maximum capacity of 51 kW. An inlet heater and choke valve ensured that the steam was superheated at the condenser inlet. At the condenser outlet, condensate drained by gravity into a receiver, and a condensate pump refilled the boilers when the condensate receiver had filled.

2.2 Test Specimen (Condenser tube)

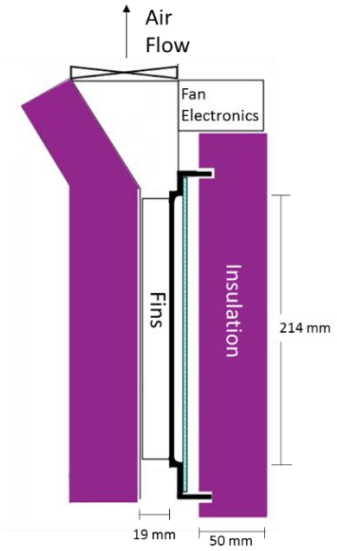

Figure 2: Facility cross-section

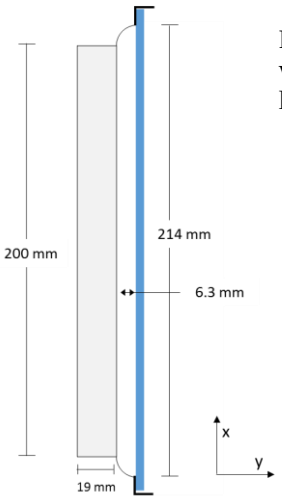

Figure 3: Condenser cross-section

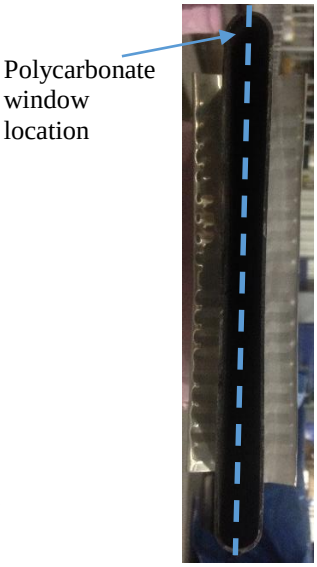

Figure 4: Picture of full tube

The flattened, carbon-steel, 10.72 m-long condenser tube with aluminum fins was cut in half lengthwise, and a 9.5 mm-thick polycarbonate sheet was attached to the open face to allow visual access. The half tube had a width of 214 mm and a depth of 6.3 mm as presented in Figure 3. The inner perimeter of the condenser, not including the polycarbonate window, was 223 mm. The fin length was 200 mm and the height was 19 mm. The axial fans were 80 mm in diameter, and were arranged to pull air upwards through the fins. Orientation of the tube, air duct, fans, and insulation can be seen in Figure 2. The un-cut full tube is pictured in Figure 4

2.3 Test conditions

Table 1: System operating parameters

Parameter	**Range**	**Uncertainty**
Inlet vapor mass flux [kg m^{-2} s^{-1}]	6.8	±1
Mass flow rate [g s^{-1}]	10.	±1
Condenser capacity [kW]	25 – 29	±3%
Air velocity (average) [m s^{-1}]	2.0	±7%
Vapor inlet pressure [kPa]	102 – 106	±0.1
Vapor inlet superheat [°C]	0.1 – 0.7	±.05
Inclination angle [°]	0.3 – 13.2	±0.4%

2.4 Measurements

Heat transfer was measured on the steam side and on the air side to provide redundant measurements. The locations of the measuring points are presented in Figure 5.

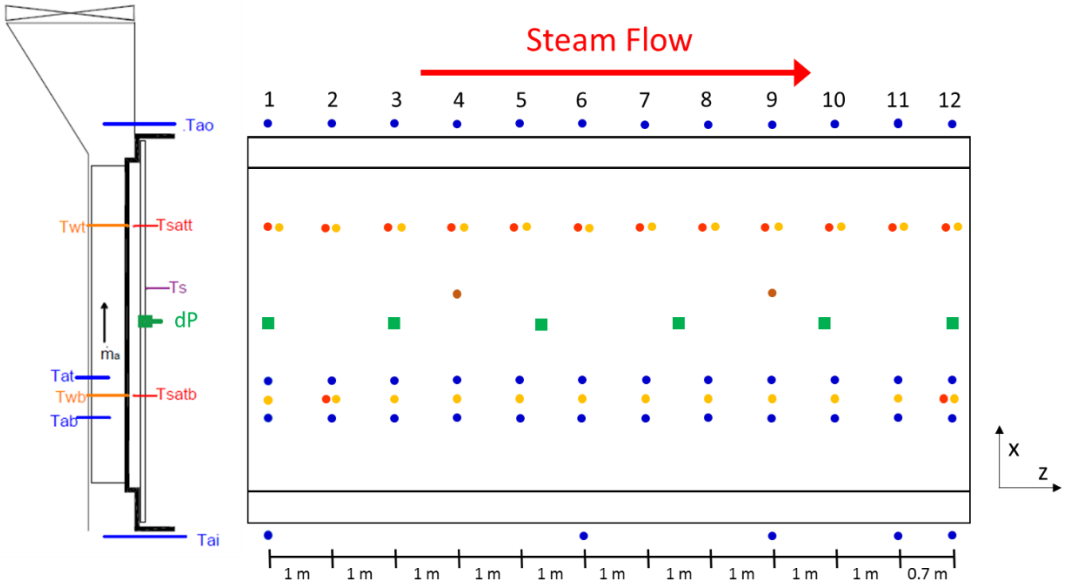

Figure 5: Schematic drawing of temperature and pressure measurement locations

Temperatures were measured at 1-m intervals along the condenser. At each point, steam saturation temperature, condenser wall temperature, air in and out temperature, and local air temperature were measured. Saturation temperature of the steam and condenser wall temperature were measured at x-locations 160.5 and 53.5 mm, in order to detect temperature gradients along the tube height. T_{amb}, T_{satt}, T_{satb}, T_s, T_{ai} and T_{ao} were measured using sheathed T-type thermocouples. T_{wt}, T_{wb}, T_{at}, and T_{ab} were measured using welded-bead 30-gauge T-type thermocouple wire. Condensate mass flow rate was measured at the receiver by weight, using a digital scale.

On the air side, the total length of the tube was divided into 11 sections (each 1 m long) for air velocity measurements. Air velocity was measured with a locally-calibrated Alnor Compuflow 8585 hot wire anemometer. Average velocity per section varied ±10% around the overall average velocity, as seen in Figure 6.

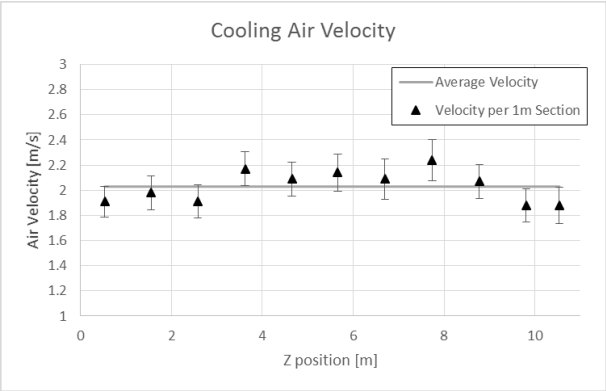

Figure 6: Average air velocity per 1m section along the condenser, measured at the inlet to the fins

2.5 Data Reduction

Air-side heat balance was determined per measurement section, *j*, based on flow rate and enthalpy difference, as in equation (3):

$$Q_{a,j} = v_{a,j}\rho_{a,j}H_a\Delta z\left(c_{p,a,out,j}T_{ao,j} - c_{p,a,in,j}T_{ai,j}\right) + Q_{a,loss,j} \tag{3}$$

$$Q_a = \sum_{j=1}^{11} Q_{a,j} \tag{4}$$

Steam-side heat balance was determined for the entire condenser from inlet and outlet conditions, as in equation (5).

$$Q_s = \dot{m}_c\left((i_{in} - i_{out})\right) - Q_{s,loss} \tag{5}$$

Assuming negligible superheat and subcooling, Q_s was simplified to:

$$Q_s = \dot{m}_c\left(i_{fg}\right) - Q_{s,loss} \tag{6}$$

Overall heat transfer coefficient U was determined from equation (7) using the uncertainty-weighted average of the steam-side and air-side heat balances, and a heat-transfer-resistance network:

$$\bar{Q} = UA \times LMTD \tag{7}$$

$$\bar{Q} = \frac{\left(\frac{1}{{u_a}^2}\right)Q_a + \left(\frac{1}{{u_s}^2}\right)Q_s}{\frac{1}{{u_a}^2} + \frac{1}{{u_s}^2}} \tag{8}$$

$$\frac{1}{UA} = \frac{1}{\bar{h}_a A_a \eta_0} + \frac{t_{st}}{k_{st}A_s} + \frac{1}{\bar{h}_s A_s} \tag{9}$$

As overall resistance could be divided into air-side, nearly-negligible conduction through the steel, and steam-side, as shown in equation (9), steam-side HTC was determined with all other variables known.

The correlation for air-side HTC for this particular geometry was provided from experimental work performed by Creative Thermal Solutions:

$$Nu = 0.1871{Re_a}^{0.5} \tag{10}$$

3. RESULTS AND DISCUSSION

3.1 Visualization of flow regimes

As diagramed in Figure 7 below, the general pattern of flow was axial vapor flow, with mixed filmwise and dropwise condensation on the tube wall. In dropwise regions, droplets of critical size would fall due to gravity, sliding along

the steel surface and cleaning the surface below of droplets. These falling droplets would almost exclusively originate at the top of the tube, as droplets lower on the surface would be continuously swept off by droplets falling from above. These falling droplets would pool in the condensate river at the tube bottom. The condensate river flowed in the axial direction, predominantly due to gravitational force. The condensate river gradually increased in depth and velocity from tube inlet to tube outlet.

From this basic description, the flow pattern could then be divided into four different flow regions along the length of the condenser: the entrance region, wavy region, transition region and stagnation region. All regions contained mixed-mode dropwise and filmwise condensation. The entrance region began at the condenser inlet and extended less than 0.5 m into the tube. This region was characterized by turbulent vapor flow. Falling droplets of condensate were subjected to significant shear stress, so they were carried downstream while falling under the influence of gravity. As a result, there was no significant condensate river in this region.

The wavy region was only present in the horizontal orientation. In this region, the condensate river had reached a depth of a few millimeters, while the vapor velocity remained high. The high vapor shear created a distinct wave pattern along the condensate surface caused by a Helmoltz instability. This region was only present in the horizontal orientation. For steeper inclinations, the condensate river was much thinner, not allowing vapor shear to overcome the condensate surface tension.

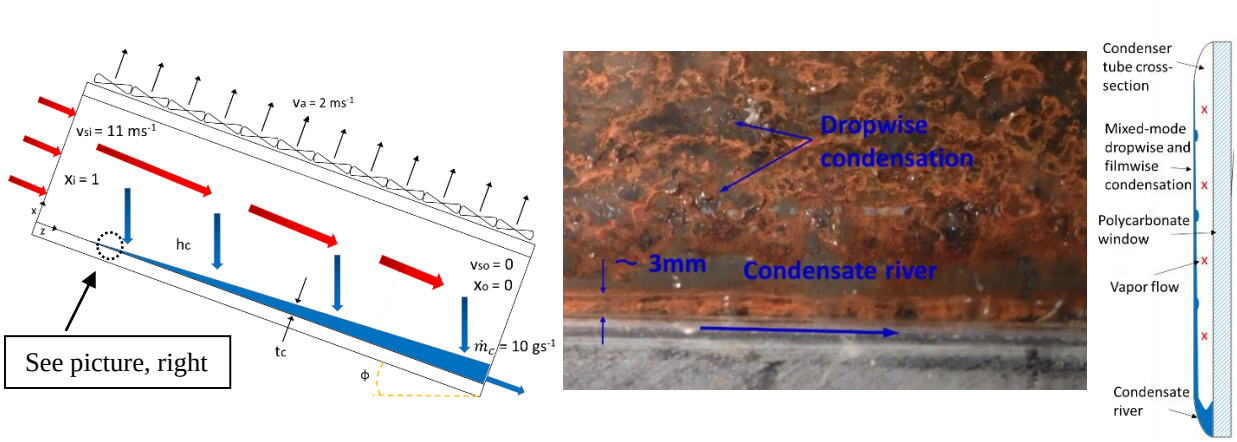

Figure 7: Diagram of vapor and condensate flow in condenser tube (L); Picture of condensate flow at z = 1m (C); Cross-sectional diagram of flow regime (R)

The transition region was characterized by a smoother vapor-condensate interface at the tube bottom. The condensate river gradually increased in depth, and the vapor flow transitioned from turbulent to laminar. As a result, the flow of condensate was almost entirely gravity driven. The falling condensate droplets fell parallel to the force of gravity, and the condensate river slowly accelerated with gravity. This region encompassed the majority of the condenser's length.

The stagnation region occurred near the tube outlet. In this region, vapor velocity fell to zero, and the condensate flow was completely dominated by gravity. Velocity and mass flow rate of the condensate river was at a maximum in this region. For the horizontal configuration, depth of the condensate river decreased in this section. For all other inclinations, the condensate river increased to a maximum at the condenser outlet.

The depth of the condensate river was also measured at five points along the condenser. Figure 8 shows that for all inclinations above the horizontal, the depth of the condensate river gradually increased along the condenser length. In addition, condensate river depth at each location decreased with increasing inclination angle. This result agrees with the trends predicted by Cheng et al. (2015). To quantitatively compare the numerical and experimental results, the cross-sectional areas of both condensate rivers were compared. This technique is necessary to account for the differing geometries between this experiment and the numerical model. In quantity of condensate in the river, the model by Cheng over-predicted the experimental results by 12%, as seen in Table 2.

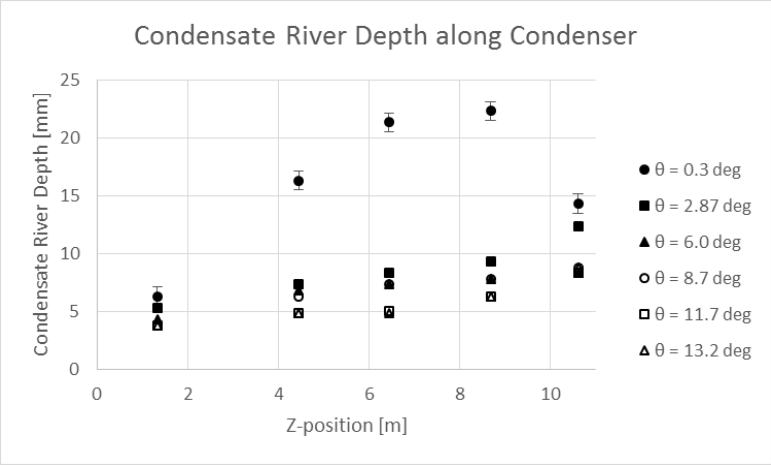

Figure 8: Depth of condensate river at discrete locations along the condenser, at six different inclination angles; error bars on 13.2º inclination only, for clarity

Table 2: Cross-sectional area of condensate river for numerical full-tube and experimental half-tube

	Full-Tube Model (Cheng et al. 2015)	**Half-Tube Experiment**
Inclination [deg]	5	6
Condensate Area [mm^2]	55.8	24.5

The depth of the condensate river affects HTC by reducing the effective steam-side area. Heat transfer by single-phase laminar convection of liquid is less than 10% of that of condensing vapor. Therefore, overall heat transfer coefficient can be assumed to be reduced by an amount proportional to the condenser area covered by the condensate river. At a given axial location, the half-tube had a perimeter of 223 mm. At an inclination of 6º, the condensate height on the steel surface was 4.3 mm at a 1.3 m axial location and 8.3 mm at a 10.6 m axial location. This corresponded to a 1.8% loss of heat transfer area between 1.3 m and 10.6 m along the condenser.

3.2 Heat Transfer Results and Discussion

For all inclinations tested, the air-side heat balance was approximately 30% greater than the steam-side heat balance. The suspected cause of the discrepancy was the difficulty in measuring air temperatures accurately. To solve this issue, the thermocouples have been moved to a location in the air duct where the temperature gradient is lower, thereby decreasing uncertainty in air-side temperature for future tests.

Figure 9 - Figure 12 show air-side heat flux at each measurement section along the condenser, for six different inclinations from 0.3 – 13.2º. Heat flux for each section is normalized to the horizontal inclination. The data show that inclination angle had the most significant effect on heat flux in the entrance region of the condenser. Inclinations of 2.9º and 6.0º showed a decrease in heat flux over the first three meters of the condenser. Heat flux over the first meter of the tube then slowly increased for angles 8.7-13.2º, reaching a maximum improvement of 6% versus the horizontal for the maximum inclination of 13.2º. The increase in heat flux over the second and third meters was not significant. The change in heat flux versus inclination was not significant for other portions of the tube, except for the 6º inclination. For this inclination, the heat flux was less than that of the horizontal for the first nine meters of the condenser tube. The portion of the tube that showed the least effects of inclination was the final two meters.

These results are surprising in that the inclination effect has been previously shown to be more pronounced for low quality and low vapor mass flux. These two variables are lowest near the condenser outlet. However, previous studies did not investigate vapor mass fluxes near stagnation, and in fact, the entrance vapor mass flux of 6.8 kg/m^2-s was below the range of operating conditions in any of the previous studies.

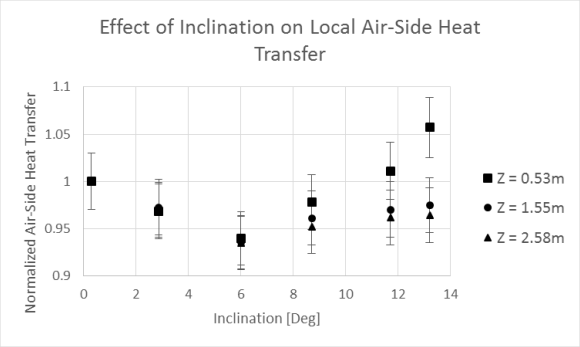

Figure 9: Heat flux over 0-3 m axial position along the condenser, normalized to the horizontal inclination

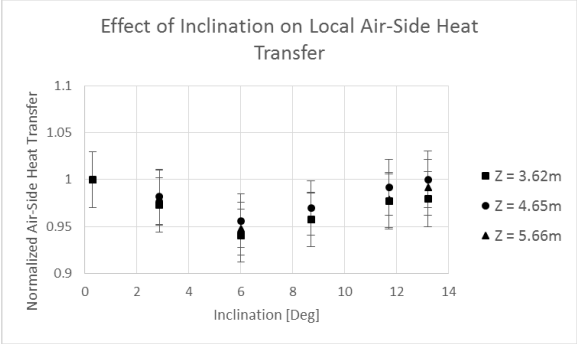

Figure 10: Heat flux over 3-6 m axial position along the condenser, normalized to the horizontal inclination

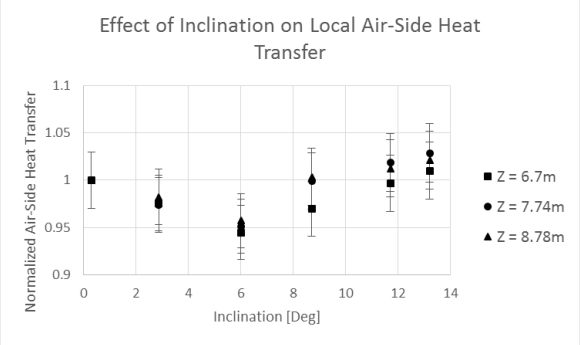

Figure 11: Heat flux over 6-9 m axial position along the condenser, normalized to the horizontal inclination

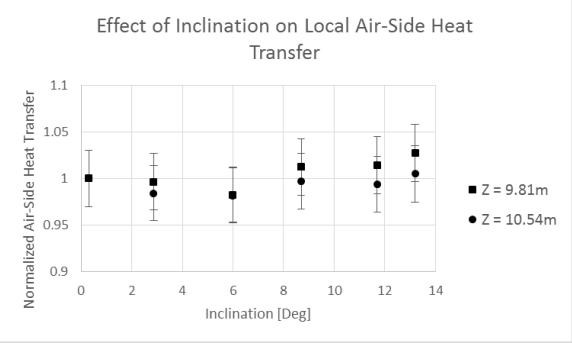

Figure 12: Heat flux over 9-10.7 m axial position along the condenser, normalized to the horizontal inclination

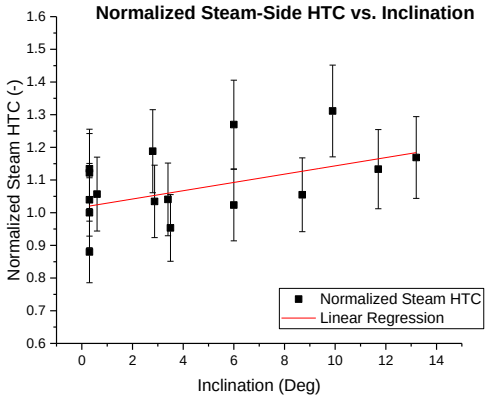

Figure 13: Steam-side HTC normalized to HTC in the horizontal inclination

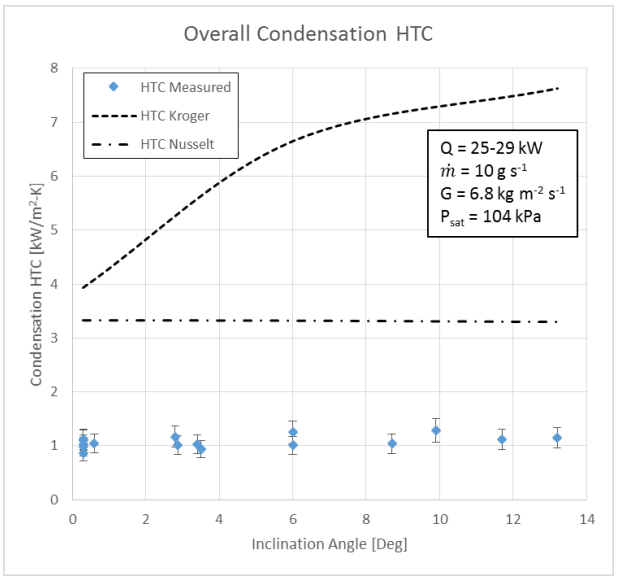

Figure 14: Measured steam-side HTC compared to predictions from Nusselt (1916) and Kröger (2004)

Based on previously-published results, steam-side HTC was expected to be a function of inclination angle, φ. The maximum overall heat transfer coefficient was expected to occur between an inclination angle of 15 and 45°. Overall steam-side heat transfer coefficient showed an increase of up to 30% versus the horizontal for inclinations of 6° and higher, depicted in Figure 13. However, the large amount of scatter in the data and the significant uncertainty made

the correlation between inclination angle and steam-side HTC weak. A linear regression of HTC over inclination angle indicated that 24% of the variation in HTC was due to inclination angle. The correlation between HTC and inclination angle was 0.49, and the slope was 0.013, with a standard error of 0.006. These data indicate that heat transfer coefficient was a function of inclination angle as expected. However, compared to the HTC predicted by Nusselt condensation (Nusselt 1916) and Kroger's correlation (Kröger 2004), the measured HTC was less than one-third of the anticipated values, as shown in Figure 14. Further work is underway to explore the reasons for this discrepancy.

4. CONCLUSIONS

Visually, the steam condensation and heat transfer occurred as expected, with mixed-mode dropwise and filmwise condensation, and a condensate river at tube bottom that increased in depth while progressing down the length of the condenser. The condensation mode and flow regime did not change with an increase in inclination from horizontal to 13.2°. However, the depth of the condensate river decreased at all positions along the condenser with an increase in inclination.

The average steam-side heat transfer coefficient increased with an increase in inclination. A 1° increase in inclination increased the heat transfer coefficient by approximately 1%. However, this relationship was obscured by uncertainty in the heat flux determination. The value of average heat transfer coefficient was lower than that predicted by either classical Nusselt condensation (Nusselt 1916), or by Kröger (2004) correlation for air-cooled condensers.

Future work will focus on extending the investigation to 90° inclination and quantifying the phenomena observed during flow visualization in order to present an accurate analytical model of the condensation heat transfer.

NOMENCLATURE

A	Area	(m^2)
c_p	specific heat	(J kg^{-1} K^{-1})
D	diameter	(m)
G	mass flux	(kg m^{-2} s^{-1})
g	gravity	(m s^{-2})
h	heat transfer coefficient	(W m^{-2} K^{-1})
H	height	(m)
i_{fg}	enthalpy of vaporization	(J kg^{-1})
i	specific enthalpy	(J kg^{-1})
k	thermal conductivity	(W m^{-1} K^{-1})
L	length	(m)
LMTD	log mean temperature difference	(^{0} C)
$\dot{m}$	mass flow rate	(g s^{-1})
Q	heat transfer	(W)
R	resistance to heat transfer	(m^2 K W^{-1})
t	thickness	(m)
T	temperature	(^{0} C)
U	overall heat transfer coefficient	(W m^{-2} K^{-1})
v	velocity	(m s^{-1})
W	width of tube	(m)
x	position along condenser height; quality	(m); (-)
y	position perpendicular to tube face (along width)	(m)
z	position along condenser axis	(m)
μ	viscosity	(kg m^2 s)
ρ	density	(kg m^{-3})
φ	inclination angle	(°)

Subscript

a	Air

b	bottom
c	condensate
f	fluid
g	gas
h	hydraulic
i	in
loss	heat transfer to ambient
o	out
s	steam
sat	saturation
sh	superheat
st	steel
t	top
w	wall

REFERENCES

Akhavan-Behabadi, M., R. Kumar, and S. Mohseni. 2007. 'Condensation Heat Transfer of R-134a Inside a Microfin Tube with Different Tube Inclinations', *Int. J. Heat Mass Transfer*, 50: 4864-71.

Chato, John C. 1960. "Laminar Condensation Inside Horizontal and Inclined Tubes." In. Boston: Ph.D. Thesis, Massachusetts Institute of Technology.

Cheng, Tongrui, Xiaoze Du, Lijun Yang, and Yongping Yang. 2015. 'Co-current Condensation in an Inclined Air-cooled Flat Tube with Fins', *Energy Procedia*, 75: 3154-61.

Kröger, Detlev G. 2004. *Air-cooled heat exchangers and cooling towers* (PennWell Books).

Lips, Stéphane, and Josua P Meyer. 2012. 'Experimental study of convective condensation in an inclined smooth tube. Part I: Inclination effect on flow pattern and heat transfer coefficient', *International Journal of Heat and Mass Transfer*, 55: 395-404.

Lyulin, Yuriy, Igor Marchuk, Sergey Chikov, Oleg Kabov. 2011. 'Experimental study of laminar convective condensation of pure vapor inside an inclined circular tube', *Microgravity Sci and Technology*, 23: 439-45.

Noie, S.H., M.R.S. Emami, and M. Koshnoodi. 2007. 'Effect of Inclination Angle and Filling Ratio on Thermal Performance of a Two-Phase Closed Thermosyphon Under Normal Operation Conditions', *Heat Transfer Eng*, 28: 365-71.

Nusselt, Wilhelm. 1916. 'Die Oberflachenkondesation des Wasserdamffes the surface condensation of water', *Zetrschr. Ver. Deutch. Ing.*, 60: 541-46.

Olivier, Stefan, Josua Meyer, Michel De Paepe, and Kathleen De Kerpel. 2015. "Measured void fraction and heat transfer coefficients during condensation." In *11th International Conference on Heat Transfer, Fluid Mechanics and Thermodynamics (HEFAT)*, 408-16.

Shah, M. M. 1979. 'A General Correlation for Heat Transfer During Film Condensation Inside Pipes', *Int. J. Heat and Mass Transfer*, 22: 547-56.

Soliman, M., J. R. Schuster, and P. J. Berenson. 1968. 'A General Heat Transfer Correlation for Annular Flow Condensation', *J. Heat Transfer*, 90: 267-76.

Traviss, D.P., W. M. Rohsenow, and A. B. Baron. 1972. 'Forced Convective Condensation in Tubes: A Heat Transfer Correlation for Condenser Design', *ASHRAE Transactions*, 79: 157-65.

Wang, Bu-Xuan, and Xiao-Ze Du. 2000. 'Study on laminar film-wise condensation for vapor flow in an inclined small/mini-diameter tube', *International Journal of Heat and Mass Transfer*, 43: 1859-68.

Wurfel, R., T. Kreutzer, and W. Fratzscher. 2003. 'Turbulence Transfer Processes in Adiabatic and Condensing Film Flow in an Inclined Tube', *Chem. Eng. Technol.*, 26: 439-48.

ACKNOWLEDGEMENTS

This material is based upon work supported by the National Science Foundation under Grant No. CBET 13-57992. The authors thankfully acknowledge the support provided by the Electric Power Research Institute, the Air Conditioning and Refrigeration Center, the University of Illinois at Urbana-Champaign and CTS – Creative Thermal Solutions, Inc.